A Novel Elliptically-Slotted Patch Antenna-based Biosensor Design

Sunday Ekpo, Vijayalakshmi Velusamy and Rupak Kharel
Department of Electrical & Electronic Engineering
Manchester Metropolitan University
Manchester, United Kingdom
Email: r.kharel@mmu.ac.uk

Abstract— **Antenna-based biosensors have attracted an increasing research interest in the biomedical and healthcare community due to their reliability, sustainability, portability, scalability and cost-effectiveness. These benefits depend on a holistic functional design and modelling of the antenna subsystem. This paper presents the design and modelling of a novel elliptically-slotted patch antenna (ESPA) based biosensor that yields a total gain of 7.5 dBi. This novel biosensing antenna is label-free, amenable to real-time embedded circuit-emulating implementations and resistant to all solvents and reagents.**

Keywords- ***biomedical sensors; biosensor; antenna based biosensor; patch antenna.***

I. INTRODUCTION

New approaches for biological cell detection are being developed to improve the biosensor characteristics such as sensitivity, smaller footprint, selectivity, integration with microfluidic devices for sample handing, reproducibility, non-invasive and rapid real-time detection. Recently, radio frequency (RF) and microwave antenna biosensors have drawn attention in the development of biological cell detection due to their numerous applications including clinical analysis, real-time monitoring (of food, water and environment) and biosecurity [1-3]. Most the intensive research interests have revolved around biological and material science fields. Antenna biosensors enable the real-time detection of the electrical and/or magnetic properties of biological materials (potentially also for bacteria like E. *coli*) at RF/microwave frequency. This approach provides a smart real time detection of biological samples without the need for biosample labelling, material intrusion and chemical transformation.

The detection principle of antenna biosensors is to sense and characterise the changes of the return loss (S_{11}) (or reflection coefficient, Γ) and the dielectric properties (i.e., relative permittivity and loss tangent) in the useable resonant RF/microwave bandwidth caused by the biosample. The dielectric properties of various biosamples at frequency 2.79 GHz such as blood, cortical bone, blood vessels, fat and muscle are given in Table 1. The development focus has been on metamaterials that can provide the needed trade-off between the practical antenna size and the designed resonant wavelength. We investigated and modelled various novel patch antenna configurations to provide the optimal sensing location for the biosample detection. The elliptically-slotted patch antenna geometry with an eccentricity of $cos\ 60^o$ (or $\sqrt{(0.75)}$) yielded the best solution for the designed antenna size and resonant wavelength. RF/microwave antenna have been considered to be more suitable for real-time biosensing due to their unique properties such as non-invasive and non-ionising radiation sensing. These make RF/microwave antenna-based biosensors the more appealing alternatives for specific transducers currently employed in the development of biosensors [1, 4, 5]. The biomedical application domain of the reported novel ESPA system can be extended to include spacecraft-borne space-based wireless biosensing devices [6, 7].

This paper is organised as follows. Section II presents the patch antenna system design including the system design parameters and the elliptically-slotted patch antenna system model. In section III, the simulation parameters, results and discussion are stated. The paper is concluded in section IV.

II. PATCH ANTENNA SYSTEM DESIGN

A. System Design Parameters

The resonant frequency, f_r, of a patch antenna is given by:

$$f_r = \frac{1}{2\pi\left(\sqrt{LC}\right)} \tag{1}$$

where the system capacitance, C, is given by:

$$C = \varepsilon_{eff}\frac{A}{d} \tag{2}$$

and ε_{eff}, the effective permittivity (i.e., the average complex permittivity of the ESPA printed circuit board (PCB) and the biosample-under-test (BUT); the inductance, L, is introduced into the feed system through the coaxial feed; A, the effective area (m^2) of the finite substrate relative to the patch and d, the dielectric separation or thickness (m). The operating (or centre-design) frequency of a microstrip (patch) antenna scales with its length, l, according to the following equation thus:

 ISBN: 978-1-61208-425-1

TABLE 1: DIELECTRIC PROPERTIES OF VARIOUS BIO SAMPLES AT 2.79 GHZ

	Density (kg/m^3)	Relative Permittivity $\varepsilon/\varepsilon_0$	Loss Tangent $\tan\delta$	Conductivity σ (S/m)
Blood	1060	57.7	0.31809	2.8581
Cortical Bone	1750	11.184	0.26642	0.46249
Fat	909.4	5.2452	0.14735	0.11996
Muscle	1059.9	52.314	0.244	1.9812
Blood Vessels	1060	42.114	0.2539	1.6596

$$f_c \approx \frac{1}{2l\sqrt{\varepsilon_o \mu_o \varepsilon_r}} = \frac{c}{2l\sqrt{\varepsilon_r}} \quad (3)$$

where ε_o is the permittivity in free space (F/m), ε_r, the relative permittivity and μ_o, the permeability in free space (H/m).

From (3), the length of the patch antenna should be equal to one-half of a wavelength within the dielectric medium.

The average complex permittivity, ε_{eff}, comprises the real and imaginary components given by:

$$\varepsilon_{eff} = \varepsilon_{eff}^{'} - j\varepsilon_{eff}^{''} \quad (4)$$

$$\varepsilon_{eff} = \varepsilon_o \varepsilon_r (1 - j\tan\delta) \quad (5)$$

$$\varepsilon_{eff} = \varepsilon_o \varepsilon_r - j\frac{\sigma}{\omega} \quad (6)$$

where $\varepsilon_{eff}^{'}$ is the lossless electromagnetic energy transmittance (EET), $\varepsilon_{eff}^{''}$, the lossy EET, δ, substrate conductivity and ω, the frequency of operation.

The EM-wave energy loss during transmittance is called the loss tangent, *tan* δ, and defined as the ratio of the lossy to the lossless EM-wave energy transmittances. The width of the patch influences the input impedance and hence, the antenna bandwidth. The larger the width of the patch antenna, the broader its bandwidth. Also, an increase in the antenna width results in a decrease in its input impedance (at the expense of a large footprint patch antenna system).

B. ESPA System Model

The CAD model of the ESPA system is created and Figure 1 shows the front view, where the elliptical slot is seen at the centre of the patch.

The substrate is a Rogers RT duroid® glass fiber reinforced polytetrafluoroethylene (PTFE) composite designed for microstrip circuit applications. The actual patch component is a substrate-centralised elliptically-slotted copper metal with a thickness of 1–1.6 mm. The ESPA system is excited with a pin, such as a SubMiniature version A (SMA) connector. The ESPA feed assembly is a coaxial cable or probe feed is from underneath through the ground plane. The outer conductor of the coaxial cable is connected to the finite ground plane and the centre conductor passes through the substrate to the patch antenna.

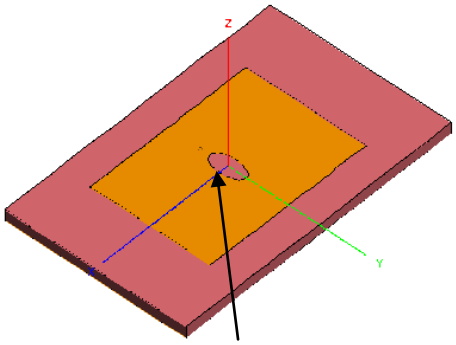

Figure 1. ESPA System (Front View)

An ESPA-based biosensor system model carries the biological sample in the elliptical slot located at the centre of the patch antenna.

III. SIMULATION RESULTS AND DISCUSSIONS

A. Slotless versus Slotted Patch Antenna

A novel ESPA was designed, modelled and simulated for biosensing applications. Table 2 shows the parameters of the ESPA system utilised for simulation. The model was simulated over finite and infinite grounds. The performance of the proposed ESPA system was compared with a conventional slotless patch antenna (CSPA). There is a considerable improvement in performance, weight, size and power consumption requirements of the ESPA design over the traditional patch antenna. Furthermore, the ESPA model allows for an integrated combinational design of metamaterials to be implemented.

TABLE 2. ESPA SYSTEM SIMULATION PARAMETERS

Model Variable	Value
f_{Max}	3.0
f_{Min}	2.6
λ_{Min}	c/f_{max}
c	$3*10^8$
P_d	$0.332\lambda_{Min}$

 ISBN: 978-1-61208-425-1

P_w	$0.468\lambda_{Min}$
S_h	$0.0287\lambda_{Min}$
F_d	$0.089\lambda_{Min}$
F_r	$0.00065\lambda_{Min}$
ε_r	2.2
R_{min}	$0.025\lambda_{Min}$
R_{maj}	$0.05\lambda_{Min}$
$tan\ \delta$	0.0004

B. ESPA Performance Analysis

Figures 2 and 3 give the reflection coefficients versus frequency for the conventional slotless patch antenna and the ESPA system respectively. The CSPA system resonates at about 2.69 GHz (finite ground) and 2.88 GHz (infinite ground) thereby yielding approximately 6.6 % difference in the resonance frequency (Figure 2). The ESPA architecture resonates at roughly 2.77 GHz (finite ground) and 2.83 GHz (infinite ground) thereby yielding a resonance difference of approximately 2.5 %. The difference in resonance becomes greater if the substrate dimensions are decreased further. In any given EM-based sensor design, a good correlation between simulated and real-life models is required. To ensure that the results of both the finite and infinite substrates improve, the geometrical size of the finite substrate must be increased to better match the infinite approximation. To obviate this requirement for reliable, small footprint and portable antenna systems for biosensing applications, the ESPA system is proposed. The centre-design frequency, f_c, of the patch antenna system is 2.793 GHz and the close-to-real-life ESPA system yields a resonance frequency of $0.993f_c$. Moreover, the simulated ESPA model indicates a good correlation and yields the same reflection coefficient of approximately -14.0 dB at the f_c (Figure 3).

Figure 4 shows the impedance magnitude of the ESPA system for biosensing applications. In any given RF/microwave system application, impedance matching is a critical requirement for system transceiver stability and/or distortionless signal applications. The finite approximation (or near-real-life) model depicts a 50-Ω impedance at 2.77 GHz. This matches the characteristic impedance (typically 50 Ω or 75 Ω) of the input port of RF/microwave transceiver systems for biosensing applications. In Figure 5, the voltage standing wave ratio (VSWR) for the closely-matched finite and infinite models of the ESPA system is approximately 4 dB at the f_c. The VSWR values at 2.77 GHz (finite substrate) and 2.83 GHz (infinite substrate) are roughly 1 dB respectively. Figure 6 shows the mismatch losses of the infinite and finite models for the ESPA system. The maximum loss for each approximation occurs at their respective resonant frequencies and agrees with the scattering-parameters analysis.

The radiation pattern of the ESPA system is illustrated in Figure 7. The fields are linearly polarised and the total gain is 5.0 dB in the vertical direction. Rectangular patch antennas are typically narrowband with a bandwidth of approximately 3 %.

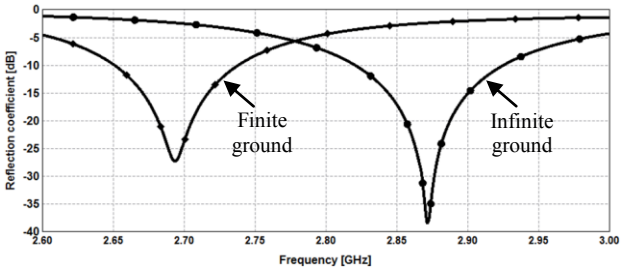

Figure 2. Reflection Coefficient versus Frequency (CSPA)

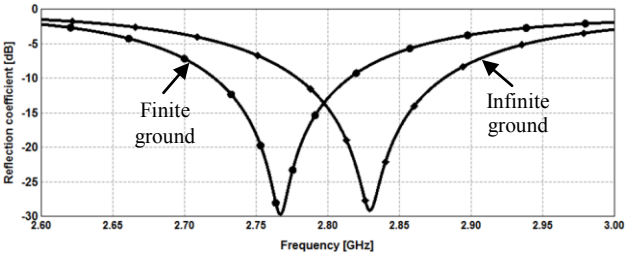

Figure 3. Reflection Coefficient versus Frequency (ESPA)

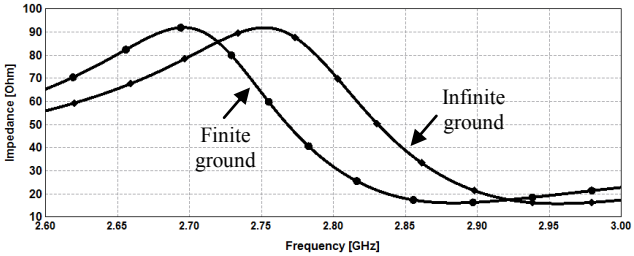

Figure 4. Impedance Magnitude of the ESPA System

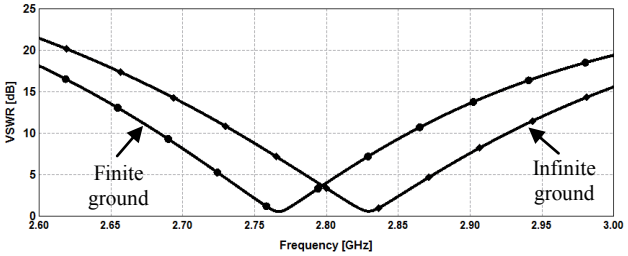

Figure 5. VSWR of the ESPA System

The ESPA was designed to operate at 2.79 GHz but it is resonant at 2.77 GHz. This frequency shift is attributed to the fringing fields around the antenna, which make the ESPA seem longer. The general design principle is to trim the patch antenna by typically 2–4 % to obtain resonance at the desired centre-design frequency. The fringing fields near the surface of the ESPA are responsible for its radiation. Equal but opposite currents flow through the ESPA and cancel the radiation due to current. The fringing fields are more bowed (extending further from patch) by a smaller value of ε_r; the smaller the value of ε_r, the better the radiation efficiency. Thus, the proposed novel ESPA is an excellent candidate for biosensing applications involving various microbes.

 ISBN: 978-1-61208-425-1

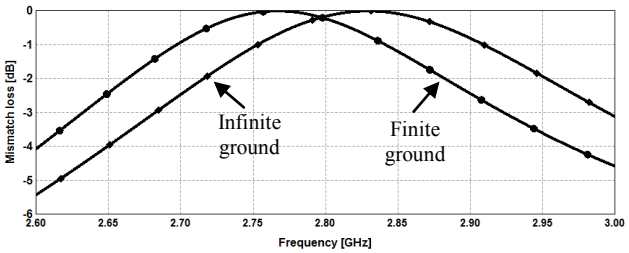

Figure 6. Mismatch Loss of the ESPA System

Figure 8 shows the radiation pattern of the ESPA system with a blood sample at 2.8 GHz with the parameters provided in Table 1 (other samples with their respective parameters can be used as well). The directivity of the antenna changes due to the presence of the sample and yields 7.5 dBi. This helps to differentiate between various biosamples and serves as a real-time biosensor for body tissues and micro-molecules.

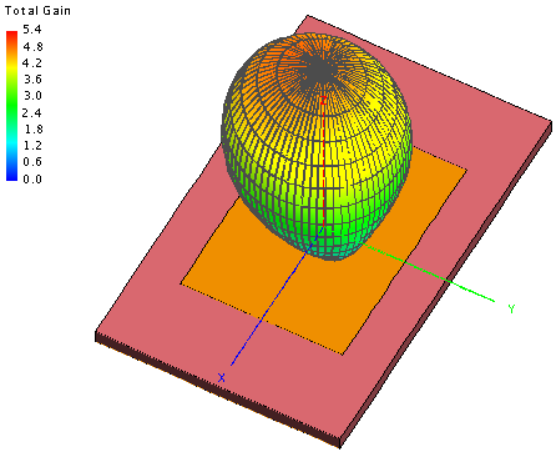

Figure 8. Radiation Pattern of the ESPA with Blood Sample at 2.8 GHz

IV. CONCLUSION

The presented novel elliptically-slotted patch antenna has the lowest electrical loss, low moisture absorption, uniform electrical properties over the operating frequencies and excellent chemical resistance. The ESPA geometry with a semi-major to semi-minor axes ratio of 2:1 and an eccentricity of cos 60^o (or $\sqrt{(0.75)}$) yielded the best solution for the designed antenna size and resonant wavelength. The ESPA system yields a total gain of 6.0 dBi, 7.5 dBi and 9.0 dBi at 2.6 GHz, 2.8 GHz and 3.0 GHz respectively. The substrate is a glass microfiber reinforced PTFE composite that can be easily integrated into real-time embedded microstrip circuit for low-cost, small footprint, low-profile and easy-to-fabricate biosensor systems applications. This novel antenna is more suitable for biosensing application as it holds a great promise in enhancing the sensitive, selective, real-time detection of low-concentration label-free and "spot-volume" biological samples.

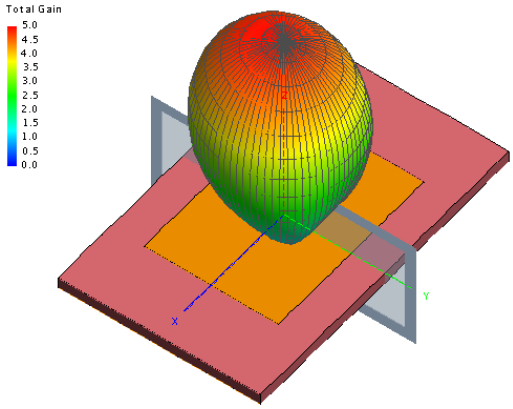

Figure 7. Radiation Pattern of the ESPA System at 2.8 GHz

REFERENCES

[1] O. Korostynska, A. Mason, and A. Al-Shamma'a, "Microwave sensors for the non-invasive monitoring of industrial and medical applications," Sensor Review, vol. 34, pp. 182-191, 2014.

[2] A. Pal, A. Mehta, M. E. Marhic, K. C. Chan, and K. S. Teng, "Microresonator antenna for biosensing applications," Micro & Nano Letters, IET, vol. 6, pp. 665-667, 2011.

[3] D. M. Elsheikh, H. A. Elsadek, E. A. Abdallah, S. Atteya, and W. N. Elmazny, "Rapid detection of blood entero-viruses using microstrip antenna bio-sensor," in Microwave Conference (EuMC), 2013 European, pp. 878-880, 2013.

[4] H. J. Lee and J. G. Yook, "Recent research trends of radio-frequency biosensors for biomolecular detection," Biosensors & Bioelectronics, vol. 61, pp. 448-459, 2014.

[5] B. Kim, S. Uno, and K. Nakazato, "Miniature on-chip spiral inductor RFID tag antenna fabricated with metal layer of standard CMOS process for biosensor applications," in Antennas and Propagation in Wireless Communications (APWC), 2011 IEEE-APS Topical Conference on, pp. 925-928, 2011.

[6] Ekpo, S. C., Adebisi, B., George, D., Kharel, R. and Uko, M., "A System-level Multicriteria Modelling of Payload Operational Times for Communication Satellite Missions in LEO," *Recent Progress in Space Technology*, Vol. 4, No. 1, pp. 67–77, June 2014.

[7] Ekpo, S. and George, D., "Impact of Noise Figure on a Satellite Link Performance," *IEEE Communications Letters*, Vol. 15, No. 9, pp. 977–979, June 2011.

 ISBN: 978-1-61208-425-1